



**IMPEDANCE and STABILITY CONSIDERATIONS  
FOR THE SNS  
PART II**

**BNL/SNS TECHNICAL NOTE**

**NO. 046**

**M. Blaskiewicz**

**August 9, 1998**

**ALTERNATING GRADIENT SYNCHROTRON DEPARTMENT  
BROOKHAVEN NATIONAL LABORATORY  
UPTON, NEW YORK 11973**

# Impedance and Stability Considerations for the SNS: Part II

M. Blaskiewicz

August 9, 1998

## Abstract

SNS Tech note # 42 is continued. Impedance estimates for pipe transitions are refined and the relative merits of aluminum versus stainless steel vacuum chambers are considered.

## Vacuum chamber transitions

In a previous note [1] the longitudinal impedance due to pipe transitions was taken to be

$$Z_{\parallel}(f) \approx -ifd\ell\mu_0/b, \quad (1)$$

where  $f$  is the cyclic frequency,  $d$  is the depth of the transition,  $\ell$  is its length, and  $b$  is the pipe radius. The associated transverse impedance was approximated as

$$Z_{\perp}(f) = cZ_{\parallel}(f)/(\pi fb^2). \quad (2)$$

In reality, the impedance is not purely reactive and it does not scale linearly with the length of the transition. The actual transitions in the SNS have yet to be fully determined so a simple model will be used. It is assumed that the beam pipe is round and has a radius that varies between 8 and 12 cm. The code abci[2] was used for the simulations. Figure 1 shows the cavity geometry and the line density of the beam used to drive it. The beam travels at the speed of light and has a Gaussian profile with  $\sigma = 10$ cm.

The actual vacuum chamber has many transitions and the lengths vary. The stepwise change in radius shown in Figure 1 yields more reflections and hence greater impedance than smooth transitions. Figure 2 shows the impedance of four different geometries with stepwise transitions. The transverse resistance vanishes below 730MHz, the cutoff frequency for TE modes in a 12cm pipe, while the transverse reactance tends to a constant value at low frequencies. Cases 2 and 4 are essentially identical below 1.1 GHz, the cutoff frequency for the TE mode in a pipe of radius 8cm. This implies that the cavities are isolated resonators below the cutoff frequency for microwave propagation down the beam pipe and the total impedance can be obtained by multiplying the impedance of one transition by 32, the number of arc dipoles. To a good approximation all the cases in Figure 2 have an inductive impedance of  $300\Omega/\text{m}$  at zero frequency. Figure 3 shows the impedance for the first three geometries shown in Figure 2 with the exception that a linear 20cm long transition was used instead of a step.

Figure 4 show the impedance for a 40cm transition. As is clear from comparing the figures, smoothing the transition greatly reduces the transverse impedance at low frequency.

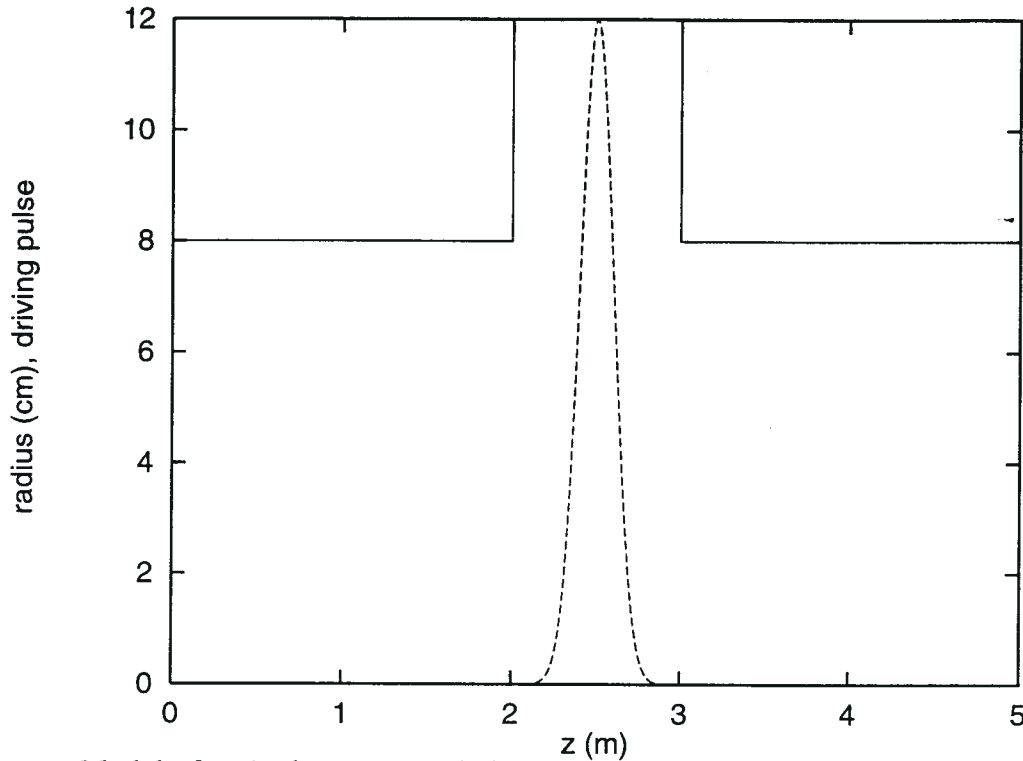


Figure 1. Model of a single cavity and the beam used to simulate the fields.

The resistive impedance is also lower for smooth transitions than for steps. The simulations shown were obtained using a wake potential of length 20m with a triangular window in the time domain. The actual resonances are much sharper than those shown for frequencies below the cutoff frequency for the TE mode, 1.1GHz[3]. The resonance width depends on the skin depth and scales as  $Q \sim d/\delta$ , where  $Q$  is the quality factor of the resonance,  $d$  is the radius of the structure and  $\delta = \sqrt{2\rho/\mu\omega}$  is the skin depth.

## Vacuum chamber material

Aluminum and stainless steel have been considered. For radio and microwave frequencies the resistivities are constant and are  $7\mu\Omega\text{cm}$  and  $72\mu\Omega\text{cm}$  for aluminum and stainless steel, respectively. The resonance lines due to vacuum chamber transitions are a factor of  $\sqrt{72/7} = 3.2$  broader for stainless steel than aluminum. For a resonance at 1GHz and assuming a line width  $\Delta f = f_{res}\delta/d$  yields resonance line widths of 4.2kHz and 13kHz. Both of these line widths are significantly larger than the frequency spread in the beam so stainless steel will be about 3 times better than aluminum, assuming a worst case resonant frequency. The resistive wall impedance scales as the square root of the resistivity so stainless steel is about three times worse than aluminum. Using coasting beam formulas for the 2MW case the resistive wall growth rates are  $\alpha_{rw} = 810\text{s}^{-1}$  and  $\alpha_{rw} = 2600\text{s}^{-1}$  for aluminum and stainless steel, respectively. However, for the AGS Booster a resistive wall growth rate

$\sim 10^3\text{s}^{-1}$  was predicted[4] using the same equations as in [1] and has never been observed. This is probably due to neglecting the damping effect of the coherent space charge tune spread, but needs further consideration. Table 1 summarizes the results.

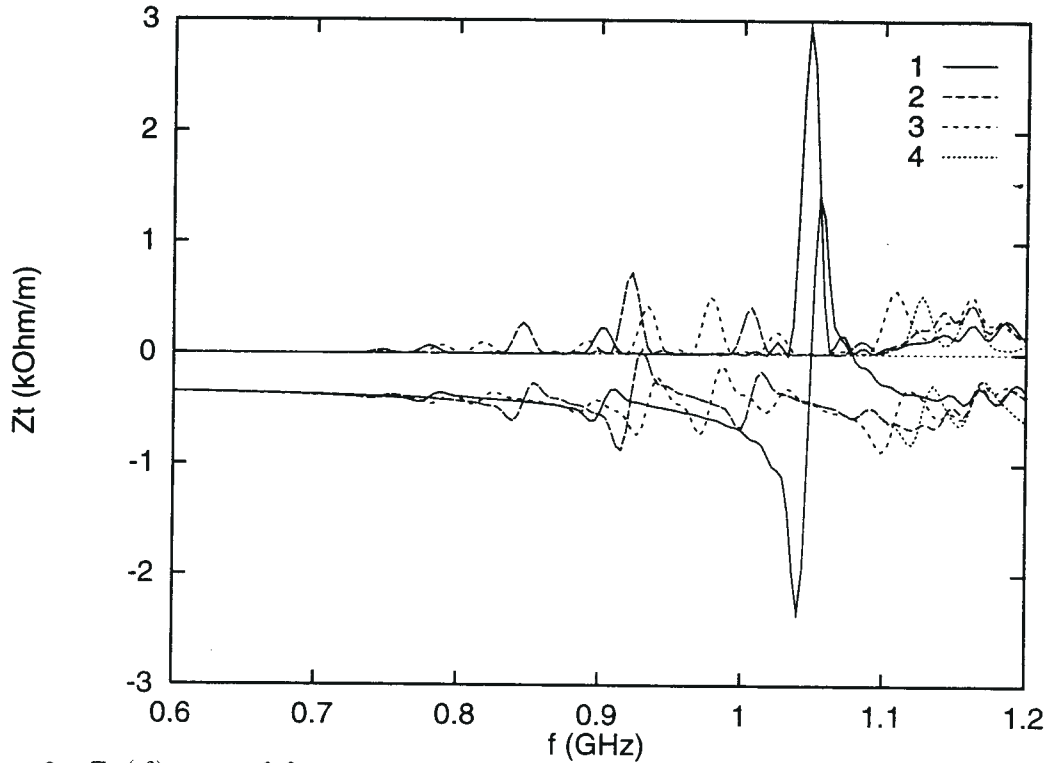


Figure 2.  $Z_{\perp}(f)$  vs.  $f$  for a pipe radius of 8cm and a cavity radius of 12cm with a step change in radius for 4 cases:

- 1) 0.5m cavity length,
  - 2) 1m cavity length,
  - 3) 2m cavity length.
  - 4) 3 1m cavities with 1m separation between cavities, final impedance divided by 3,
- In all 4 cases the transverse impedance at zero frequency was  $-i300\Omega/\text{m}$ .

quantity	current estimate	old estimate
$Z_{\perp}$ from step transitions	9.6k $\Omega/\text{m}$	360k $\Omega/\text{m}$
$Z_{\perp}$ from 20cm transitions	3.2k $\Omega/\text{m}$	
$Z_{\perp}$ from 40cm transitions	1.9k $\Omega/\text{m}$	
resistive wall growth rate: stainless	2600s $^{-1}$	2600s $^{-1}$
resistive wall growth rate: aluminum	810s $^{-1}$	

Table 1. Summary of old and new impedance estimates, a blank indicates that no estimate was made.

An additional consideration involves the production of secondary electrons. Figure 5 shows the electron yield versus incident electron energy for the two cases [5]. For small incident energies the yield must go to zero, but the data are difficult to obtain. The effect of secondary emission on the beam

via the electron proton instability has not been calculated but preliminary numerical results ignoring secondary emission show that the beam will be stable. The same simulations using parameters for the PSR showed no instability either. Therefore, if the PSR instability is an electron proton instability then secondary emission is a critical element and reducing secondary emission can only help. Given the lack of a resistive wall instability in the AGS Booster and the difficulties at the PSR, stainless steel is a better choice than aluminum.

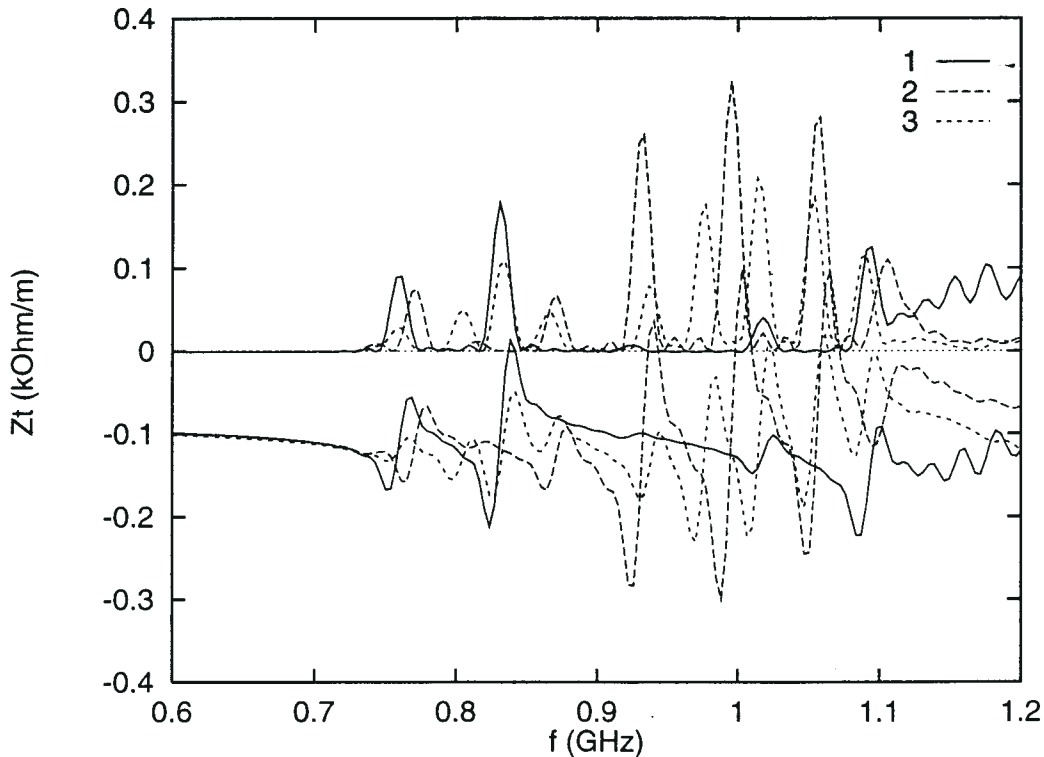


Figure 3.  $Z_{\perp}(f)$  vs.  $f$  for a pipe radius of 8cm and a cavity radius of 12cm with a 20cm transition length for 3 cases:

- 1) 0.5m cavity length,
- 2) 1m cavity length,
- 3) 2m cavity length.

## References

- [1] M. Blaskiewicz, Impedance and Stability Considerations for the SNS, SNS Tech Note # 42, 1998.
- [2] Y.H. Chin, ABCI version 9.2.1, (1995).
- [3] Jackson, *Classical Electrodynamics*, Wiley, (1975).
- [4] Booster Project Design Manual, section 2.7, 1989.
- [5] Noel Hilleret, private communication.

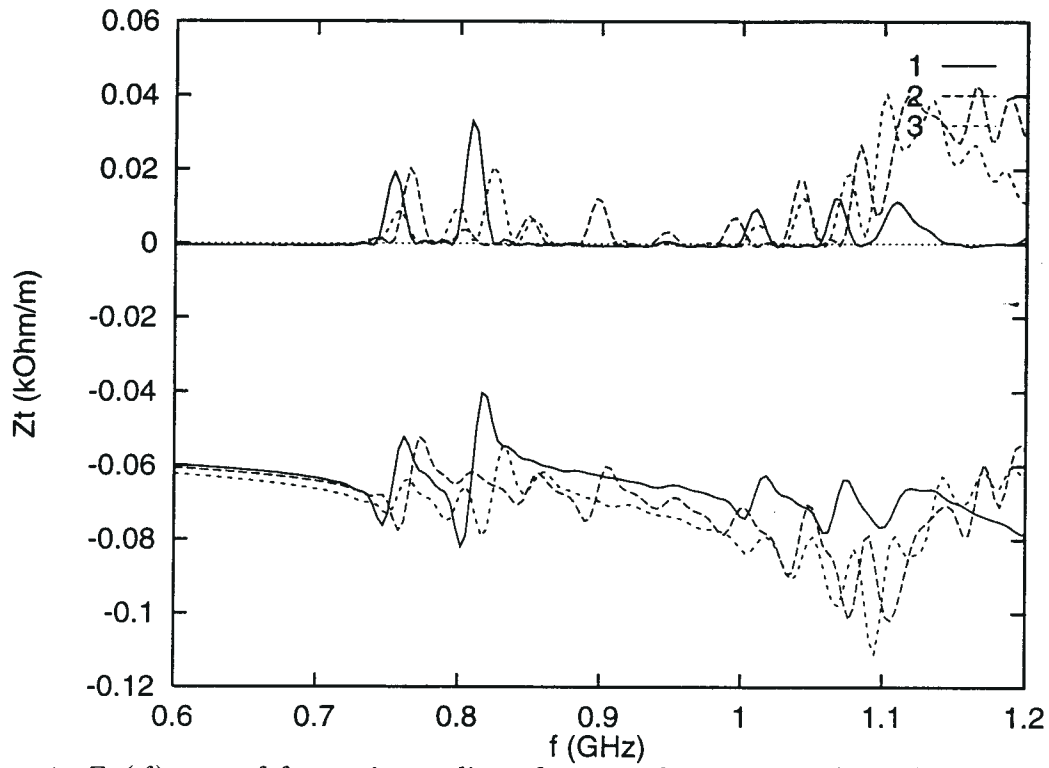


Figure 4.  $Z_{\perp}(f)$  .vs .  $f$  for a pipe radius of 8cm and a cavity radius of 12cm with a 40cm transition length for 3 cases:

- 1) 0.5m cavity length,
- 2) 1m cavity length,
- 3) 2m cavity length.

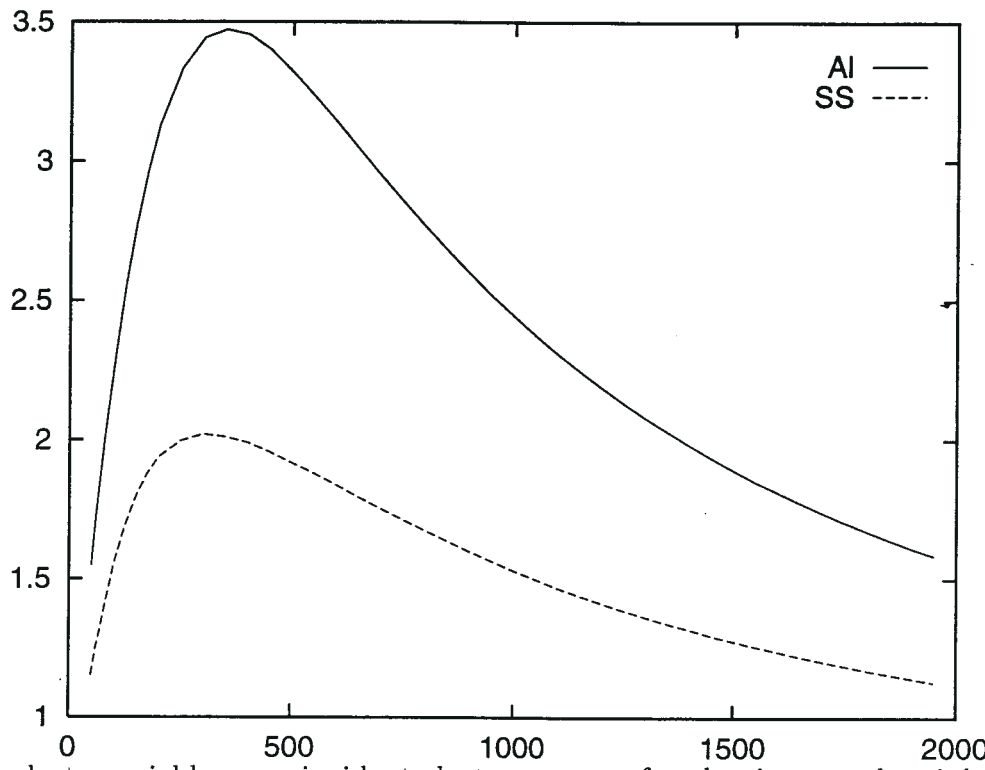


Figure 5. electron yield versus incident electron energy for aluminum and stainless steel.